Six-Year Trend of Concentrations of Ultrafine Particles Six Kilometres Away from a Major German Airport

Holger Gerwig[1], Wolfram Birmili[1], Kay Weinhold[2], Honey Dawn Cotecson Alas[2], Alfred Wiedensohler[2], Wilma Travnicek[1]

[1]German Environment Agency (UBA), Dessau-Roßlau, Germany
[2]Leibniz-Institut für Troposphärenforschung e.V. (TROPOS), Leipzig, Germany

Correspondence to: Holger Gerwig (holger.gerwig@uba.de)

Abstract. Ultrafine particles play a crucial role in the atmosphere, both as a source of larger particles and as a factor influencing human health. We analysed hourly particle number size distributions collected during 2015–2021 from an urban background station in the Rhine-Main area in Germany, focusing on potential particle sources and multiannual trends. The site is influenced by diffuse regional sources such as motor traffic and domestic heating, as well as Frankfurt Airport, located at a distance of 6 km. The average total particle number concentration (TNC, size range 10–500 nm) was 9.4×10^3 cm^-3. TNC maxima were observed in diurnal cycles at 07:00, 13:00, and 21:00. The midday peak was more distinct during the warm season and dominated by nucleation mode particles (NUC, 10–30 nm), suggesting photochemical particle formation as a source. When the wind was blowing from Frankfurt airport, a 2.5-fold concentration average in NUC was observed compared to other directions (11.2×10^3 cm^-3 and 4.3×10^3 cm^-3, 2015–2021). In 2020, during traffic restrictions related to the COVID-19 lockdown, TNC downwind of the airport was 40–60% lower compared to the average of the four years before. Overall trend analysis for 2015–2021 yielded consistent downward trends for TNC (-2%×year^-1), atmospheric particulate matter PM_{10} mass (4%×year^-1) and nitrogen dioxide NO_2 (-5%×year^-1). While our observations of particle number size distributions show general similarities to other Central European observations, the effect of winds from Frankfurt Airport as a particle source is most prominently seen in the range 10–30 nm. The airport's role as a source of NUC and the rise in flights from 2015 to 2019 may be the cause of lower decline rates when compared to other locations.

1. Introduction

Atmospheric aerosol and air quality science have achieved major advances in recent years, but important questions remain. Specific challenges concern the sources of ultrafine particles (UFP; particles with a size < 100 nm in diameter), their further processing in the atmosphere and finally, their impacts on climate and human health. The adverse health effects of UFP have not been fully ascertained, mostly due to a lack of sufficient long-term studies (Cassee et al., 2019; Ohlwein et al., 2019). Nevertheless, the WHO has forwarded concrete atmospheric UFP concentrations as a "good practice statement" in its latest report (WHO, 2021). It is worth to note that WHO defines UFP as a total particle number concentration (TNC) with a lower size limit of 10 nm or less and an open upper end. The WHO considers a 24-hour mean of TNC < 1,000 cm^-3 as "low concentrations". Values of TNC > 10,000 cm^-3 are classified as "high concentrations". The new EU Air Quality Directive 2024/2881 (Anon, 2024) includes the requirement to measure Particle Number Concentration (PNC) and Particle Size Distribution (PSD).

Atmospheric UFP and the particle number size distributions (PNSD) may occur in considerable variation in the atmosphere due to rapid dynamic processes such as particle nucleation from gas-phase compounds, subsequent particle growth, coagulation, deposition, and activation as cloud condensation nuclei (CCN) (Bousiotis et al., 2021; Yao et al., 2018). As shown by stationary and mobile observations, large and frequent spatio-temporal gradients occur in urban atmospheres (Trechera et al., 2023; von Schneidemesser et al., 2019). The overall factors influencing UFP concentrations include time of day, wind direction, season, wind speed, temperature and solar radiation (von Bismarck-Osten et al., 2013). The mixed layer height (MLH) (Emeis et al., 2008) is a critical factor in the dispersal of any kind of pollutant near the ground. Over continental areas, the mixed layer is typically more shallow at night-time and during the winter season (Ma, 2013; Geiss, 2017), effectively trapping pollutants emitted near the ground.

Combustion is a major source of UFP including a range of individual sources such as the engines of vehicles, aircraft, and ships, as well as power and heat generation plants and domestic heating. Airborne measurements suggest that plumes from industrial plants contribute to 10-40% of background UFP in Germany (Junkermann et al., 2016). The effects of road traffic are evidenced by numerous studies in urban areas (e.g., Wehner et al., 2002; Gani et al., 2021).

A contrasting phenomenon is secondary new particle formation (NPF), i.e., nucleation from gaseous precursors and subsequent growth into larger diameters. This process is typically driven by the photochemical generation of the combination of one or more of the following compounds: sulphuric acid, amines and organic molecules. This may occur simultaneously over large spatial areas and is independent from combustion-driven UFP emission (Kerminen et al., 2018). In a continental atmosphere, combustion-derived UFP and (secondary) NPF may overlap in observations, making a separation of the contributions difficult. Ma and Birmili (2015) attempted to separate these contributions based on multiple-site observations and concluded that secondary NPF contributed up to 30% of nucleation mode particles in an urban area. Clustering analysis identified NPF as the most important source for 16% of particle size distributions in Southern Europe (Brines et al., 2015). Several studies have intensely discussed the source apportionment of UFP (Garcia-Marlès et al., 2024; Hopke et al., 2022; Trechera et al., 2023; Vörösmarty et al., 2024).

Aircraft engines emit a large fraction of UFP as nucleation mode (NUC hereafter) particles (Brock et al., 2000). Not surprisingly, airports are significant sources of elevated UFP as well, particularly in the NUC range (Lorentz et al., 2019; Stacey, 2019; Rivas et al., 2020). NUC formation after aircraft exhaust involves a dynamic interplay

of chemical species. Sulphuric acid often acts as the primary nucleating agent (Schneider, 2005). Lower fuel sulphur content increases the relative contribution of organic compounds to NUC formation (Yu et al., 1999). Jet engine lubricants contribute to the UFP mass fraction (Ungeheuer et al., 2021). Atmospheric observations downwind from airports typically show elevated NUC concentrations most pronounced at about 5–10 km: Los Angeles showed 4-fold increases at 10 km (Hudda et al., 2014). Amsterdam exhibited 3-fold increases at 7 km (Keuken et al., 2015). Boston demonstrated 1.6 to 3-fold increases at 5 km (Hudda et al., 2018). Zurich modelling suggested 2 to 10-fold increases at 3 km (Zhang et al., 2020). London measurements revealed 10-fold increases at 1.2 km (Masiol et al., 2017). At distances exceeding 20 km, tower measurements show a shift towards Aitken mode particles (AIT, 30–100 nm). This shift reflects particle growth from NUC to AIT over several hours (Harrison et al., 2019; Keuken et al., 2015).

Data on atmospheric UFP have been collected over long enough time periods to identify trends. Long-term observations in North America suggest an increase in UFP over time (Chen et al., 2022). In Germany and Europe, however, decreasing trends were observed (Sun et al., 2020; Trechera et al., 2023). This decrease was associated with efforts on air quality control, although these studies did not explicitly investigate the influence of aircraft emissions.

This work presents new PNSD data from an urban background station in the Rhine-Main area of Germany, collected between 2015 and 2021, and builds upon previous research into UFP in the vicinity of FRA (Gregor et al., 2015). Our objective is to examine the impact of anthropogenic sources on local air quality. In particular, we focus on NUC and UFP concentrations from Frankfurt Airport at a distance of 6 km, considering the impact of time of day, season and wind direction. We also assess the specific impact of the lockdown period during COVID-19 pandemic, with its reductions in traffic (Putaud et al., 2021). To our knowledge, this is the first study to examine the impact of an airport on a downwind site over a six-year period.

Figure 1. Location of stations: LAN provided data on TNC, NUC, AIT, and ACC. DAR, FFM_AP, and LAN_TC provide auxiliary data. ©OpenStreetMap contributors 2025. Distributed under the Open Data Commons Open Database License (ODbL) v1.0.

2. Methods

2.1. Study area

This study is based on atmospheric measurements in the Rhine-Main metropolitan region (2.8 million inhabitants), including the city of Frankfurt (Main). An essential feature is Frankfurt Airport (FRA), which ranked 4th to 6th in Europe with regard to passenger volume during 2015-2021. Observations were made at one site for PNSD and three other sites for auxiliary observations, shown in Fig. 1. For the exact positions of the sites, see Tab. 1.

For this study, we used PNSD data from the years 2015-2021 at LAN, excluding 2016 resulting in a 6-year trend analysis. We excluded 2016 due to its low data coverage (<55%). PM concentration measurements at LAN lasted from January 1, 2019 to December 31, 2021.

Table 1. List of air quality sites supplying datasets to this study, with location and type of environment. Coor., coordinates; Alt., altitude; UB, urban background; Met, meteorological parameters; TC, traffic count; PNC, particle number concentration.

Acronym	City (station name)	Parameters	Station type	Station Code	Coor.; (Alt., m a.s.l.)
LAN	Langen Paul-Ehrlich-Str. 29	PNSD, PNC, Solar radiation, T, rH, p, wd, ws (PM10, PM2.5, PM1 in 2019-21)	UB	DEUB052[1] DE0065B[2]	50.00 N, 8.39 E; (144)
DAR	Darmstadt Rudolf-Müller Anlage	PM10, SO_2, NO, NO_2, O_3, CO	UB	DEHE001[1]	49.87 N, 8.66 E; (158)
FFM_AP	Frankfurt Airport	wd, ws	Met	DWD1420	50.23 N, 8.52 E; (100)
LAN_TC	Langen Traffic Count, B486	counts of cars and heavy-duty vehicles	TC	BAST6221	49.99 N, 8.65 E; (130)

[1]EU station Code, [2] EBAS-station codes.

- LAN (Langen) is the main observation site for particle number size distributions (PNSD). The urban background site is on the roof of the laboratory building of the German Environment Agency, or Umweltbundesamt (UBA), in Langen. This is a mixed business/residential neighbourhood 1.5 km northwest of the city centre (approximately 40,000 residents). It lies 15 km south of Frankfurt (Main) and 15 km north of Darmstadt. Site classification and details can be found in Birmili et al., 2016 and Sun et al., 2020 for further information. Significant roads are located in the vicinity of the site. These include 500 m to the south (B486 federal road, ca. 24,000 vehicles x day^-1, 6% heavy-duty vehicles), 3 km to the east (A661 motorway, ca. 70,000 vehicles x day^-1, 6% heavy-duty vehicles), and 4 km to the west (A5 motorway, ca. 130,000 vehicles x day^-1, 11% heavy-duty vehicles). An overview of parameters is given in table 1 and additional information in table S1. In addition to the PNSD data from LAN, we also used data from three additional observation sites:
- **DAR** (Darmstadt) is an urban background site to supply general air quality data in the city of Darmstadt (Rudolf-Mueller-Anlage), 15 km south of LAN and 18 km southeast of Frankfurt Airport. It is operated by the governmental authority Hessian Agency for Nature Conservation, Environment and Geology (HLNUG) (HLNUG, 2023a). Hourly concentrations are provided: NO, NO_2, CO, O_3, SO_2, and PM_{10} mass. The longer distance, particularly between the two stations LAN and DAR, made it difficult to adequately compare the gaseous pollutants to PNSD.

- **FFM_AP** (Frankfurt Airport) provides data on meteorological parameters. It is situated on flat grassland at the edge of the airport field. It is operated by the German Weather Service (DWD). Because buildings and building components to the northeast were shaded by winds, we preferred the weather parameters from FFM_AP over LAN. For completeness, wind roses for both LAN and FFM_AP for 2015–2021 are given in the supplement (see Fig. S1).
- **LAN_TC** (Langen Traffic Count) is an automatic counting station for vehicular traffic at the edge of the B486 federal road, 1 km south of LAN. It is operated by the German Federal Highway Research Institute (BAST, 2023).

It is expected that traffic emissions from major highways and local roads less than five kilometres away, whose traffic count is recorded at the nearby station LAN_TC, will affect LAN measurements. Urban emissions such as domestic heating and limited industrial sources can be found in the surroundings of LAN. Natural gas is primarily used for domestic and commercial heating, with residential wood combustion likely to have increased recently. Residential wood combustion has been identified as the most important source of VOCs during winter in a city (Languille et al., 2020). There is a gas-fired power plant (DFS Energy Centre) 500 m to the north with 120 MWh fuel consumption per year (DFS, 2022).

A 430 MW coal-fired power plant in Frankfurt (Main), 11 km north, may be the primary source of SO_2 emissions. In Hesse, industry accounts for over 70% of the total 2000 txa^-1 SO_2 emissions, with aircraft burning kerosene up to 300 m above ground contributing less than 10% (HLNUG, 2023b). The transport of polluted air from Eastern Europe to Eastern Germany is a major source of PM10 mass (50%) and SO_2 (van Pixteren et al., 2019).

2.2. Instrumentation

The following instrumentation was used for atmospheric measurements at the main observation site, LAN:

Particle number size distributions (PNSD) were measured by a Scanning Mobility Particle Size Spectrometer (MPSS). We used a TSI MPSS (TSI Inc., USA, model 3936), modified by the Leibniz Institute for Tropospheric Research (TROPOS), Leipzig. The original TSI instrument was augmented with additional hardware and software from TROPOS, and Nafion® dryers were installed in the system for aerosol and sheath air conditioning. We used the negative high voltage of the differential mobility analyser (DMA). As a condensation particle counter (CPC), TSI model 3010 was used before Nov 2016, and TSI model 3772 (both with a Dp50 = 10 nm) afterwards. An X-Ray neutraliser (TSI model 3087) was used for bipolar charging of ambient aerosols. Prior to size classification, the aerosol was dried below 50% relative humidity (RH), as opposed to the optimal 40% RH (CEN, 2020). In this instance, hygroscopic characteristics and other water uptake processes may have caused the particles to grow, resulting in larger particle sizes. Smaller particles than 10 nm also grow and would therefore lead to an even higher proportion of NUC. Humidity was between 40 and 50 percent of the time, particularly during the summer months. After multiple charge inversion, the MPSS provides PNSD across a particle size range of 10-500 nm. Regular quality control was performed in association with the World Calibration Centre for Aerosol Physics (WCCAP), Leipzig, Germany. A Catalytic Stripper (Catalytic Instruments, CVF500) operating at 400°C was used since mid-2016 to remove gas-phase hydrocarbons (1-butanol) from the exhaust of the CPCs. To provide standardised sampling conditions, a PM_1 mass inlet (Digitel AG and sampling line PSE1, Riemer) was used at a total flow of 33 L min^-1, heated to 25°C. The temperature in the measurement container ranged between 20°C and 25°C, as controlled by a combination of air conditioning and heating. Although direct solar radiation heated the sampling line to 31°C during the summer, the aerosol was cooled to the temperature of the

measurement container air as it passed through the sampling line and Nafion® dryers. As a result, the PNSD's temperature range of 5°C was ignored throughout the year. For more information, see Tab. S1. We are aware that inlet heating has not been recommended since 2020 and that the PM1 mass inlet should be PM2.5 or PM10 (CEN, 2020). We recommend that future studies meet the UFP measurement requirements of ACTRIS and CEN (CEN, 2023, 2020), as well as Wiedensohler et al., 2018, 2012. Therefore, in future we will use an adapted MPSS of TROPOS for PNSD from 10 to 800 nm, including improved sampling according to CEN. Then, we will dry the sampled aerosol below 40% RH and use a PM2.5 inlet as is recommended in the Service Tool 1 prepared within the "Research Infrastructures Services Reinforcing Air Quality Monitoring Capacities in European Urban & Industrial AreaS" EU-project (RI-URBANS, 2024).

The meteorological parameters (FFM_AP) and the concentrations of PM mass and gaseous pollutants (DAR) were recorded at the corresponding nearby stations using instruments that comply with European legislation standards. All data obtained were averaged to hourly values.

2.3. Data treatment

The non-parametric Mann-Kendall test (Kendall, 1975; Mann, 1945) was used to determine an increasing or decreasing trend over time. In the presence of a statistically significant trend, the amount was quantified by the Theil-Sen slope. This is the median of all possible slopes between the data pairs (Sen, 1968; Theil, 1992). To accomplish this, monthly data series spanning more than 6 years were aggregated with a 30% threshold and de-seasonalized using the seasonal decomposition of time series by loess (Cleveland et al., 1990). It should be noted that a 6-year time series for identifying trends is quite short. Data preparation and statistical analysis were carried out with R (v3.6.1, (R Core Team, 2019)) and the Openair package (v2.18-2, 2024-03-11) (Carslaw and Ropkins, 2012). To better compare the contributions to exposure to an air pollutant between the modes, we have divided the 10° cut wind sectors into 20° or 30° sectors: northeast (NE) 40-60°; northwest (NW) 290-310°; southwest (SW) 190-220°. The TNC in this study has three particle modes: nucleation (NUC: 10-30 nm), Aitken (AIT: 30-100 nm), and accumulation (ACC: 100-500 nm). The specific size range for NUC often depends on the instrumentation used for measurement, the specific scientific question being addressed, and the environment being studied (e.g., urban, remote, marine). It is currently defined as 3-25 nm (Wehner et al., 2005) but with higher lower and upper limits for modelling aerosols of 10-40 nm (Lupascu et al., 2015). In this study, we defined NUC with a lower limit of 10nm based on the equipment used (Trechera et al., 2023), and an upper limit of 30 nm to capture as well the slight overlap of nucleation mode particles with Aitken mode particles.

In the LAN data set 2015-2019, high particle number concentrations were detected in the finest size fractions (Trechera et al., 2023). A measurement in the 10 nm range places high demands on instrumental detection, as the CPC used has a low detection efficiency in that range. Therefore, instrument-to-instrument variability has been observed to be higher below 20 nm than above this size (Wiedensohler et al., 2012). However, this higher variability has considerable effects, especially on the number concentrations in NUC.

We are aware that the proportion of larger particles in the 500–800 nm range is not measured in accordance with CEN guidelines (2020).

3. Results and Discussion

3.1. Particle number concentrations of size fractions

Table 2 presents the multiannual statistics of TNC-derived PNSD (10-500 nm). The corresponding data for the year 2021 is given in Table S3. The median TNC was 8.2×10^3 cm^-3 (7.9×10^3 cm^-3 in 2021). The NUC range had the highest fraction of TNC (median 3.7×10^3 cm^-3, 44% 2015-2021; 3.9×10^3 cm^-3, 49% in 2021). These values are within the typical range of other urban background stations in Germany and Europe (Sun et al., 2020; Trechera et al., 2023). The highest 1% of hourly TNC ranged from 31 to 290×10^3 cm^-3 for the entire period and from 27 to 54×10^3 cm^-3 in 2021.

Table 2. Hourly Concentrations at Langen (LAN) 2015-2021 (2016 excluded) for nucleation, Aitken and accumulation mode particles (NUC, N10-30; AIT, N30-100, and ACC, N100-500) and total number concentration (TNC, N10-500). Data coverage in % per annum (p.a.).

PNC in cm^-3	Min.	1perc	Median	Mean	SD	99perc	Max	coverage (%)
TNC	572	1 806	8 286	9 352	6 082	30 930	289 689	71
NUC	79	572	3 699	4 996	5 082	24 349	271 376	71
AIT	112	441	2 772	3 191	2 009	9 738	17 915	71
ACC	22	130	1 009	1 165	792	3 615	21 547	71
N_{30-500}	141	610	3 886	4 356	2 553	12 109	30 397	71

3.2. Temporal trend of TNC

Figure 2 displays the temporal trend of seasonal mean TNC at LAN from 2015 to 2021, with seasons defined as 3-month periods (winter: December-February).

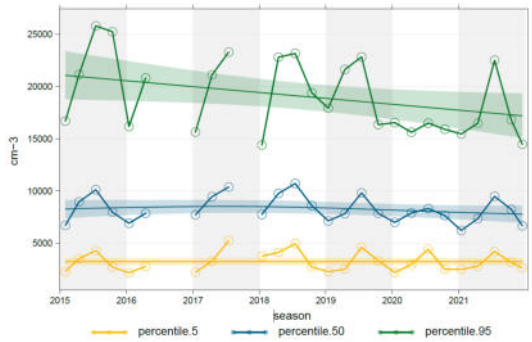

Figure 2. Trend of seasonal means of TNC from 2015 to 2021 at LAN.

The regression line (computed using R) is shown without statistical parameters to maintain methodological clarity, as linear regression is applied here while the Theil-Sen estimator is used in subsequent figures. The moving average reveals a decreasing trend for the 95th percentile, with a pronounced 25% drop in spring 2020. The drop of 25% in 95th percentile in spring 2020 (Fig. 2) corresponded to the COVID-19-lockdown-related decrease in traffic. lLandings and take-offs (LTO) decreased by 70% (Schultheiß-Münch et al., 2022) (s. 3.6) and car traffic on motorways by 16% (BAST, 2023) in 2020 compared to 2019 for car traffic (at LAN_TC) and 2015-2019 for airports. Several studies have examined the environmental impacts of traffic restrictions during the COVID-19 lockdown. In Spain, COVID-19 lockdown restrictions reduced traffic intensity by up to 80%, resulting in lower levels of combustion-related pollutants NO_2, CO, and SO_2 (Putaud et al., 2021; Querol et al., 2021).

Figure S2 shows annual box plots for TNC to complete the picture. The yearly medians confirm the general downward trend.

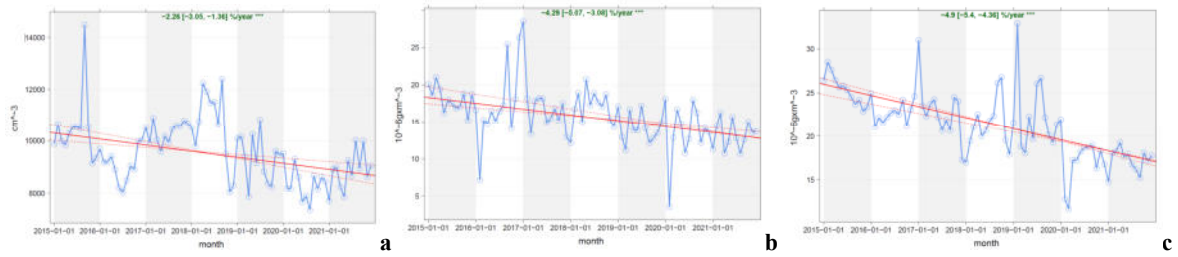

Figure 3a-c Theil-Sen trend (deseasoned) for monthly means from 2015 to 2021 for all wind directions for (a) LAN: TNC, DAR: (b) PM10, and (c) NO2.

To quantify long-term changes, we applied Theil-Sen trend analysis (see Sect. 2.3) to monthly means of daily values from 2015 to 2021 (Table S6). For better representation, Fig. 3 shows trend lines according to Theil-Sen (s. 2.3) from 2015 to 2021 on the basis of monthly means of daily mean values (cf. Tab. S6). The trend for TNC (Fig. 3a) yielded a highly significant (P<0.001) decrease of -2.3% per annum (p.a.). Even for the shorter period of 2015–2019 when excluding year 2020 as a special year of pandemic-caused reductions, the trend was still -1.9 % p. a. but less significant (P<0.05) (cf. Tab. S6). Trend analyses for an earlier period (2009-2018) at German Ultrafine Aerosol Network (GUAN) stations in Germany showed a stronger decrease between -2.6% to -6.3% p.a. for TNC (20–800 nm) (Sun et al., 2020).

Other components also showed a highly significant (P<0.001) decrease, with even higher rates: PM10 -4.3% p.a. (Fig. 3b) and NO_2 -4.9% p.a. (Fig. 3c). In contrast, some components showed a significant (P<0.01) increase: CO 3.5% p.a., ozone 1.5% p.a. (cf. Tab. S4).

When considering Tab. S4 the decrease for the different particle size ranges was the highest for NUC -2.9% p.a. at P< 0.001 (2015-2021). The decrease was lower for AIT -2.0% p.a. (2015-2021). ACC showed no significant trend or even showed an increase of 3.3% p.a. 2015-2019. Overall, the decrease in TNC seems to be associated primarily with a decrease in the subfraction NUC. This decrease is in line with decreasing trends in other combustion-related compounds of mainly anthropogenic origin, such as NO_2, PM_{10} and cf. Tab. S4 NO and SO_2. In contrast, CO, another combustion-related pollutant, increased as well as ozone.

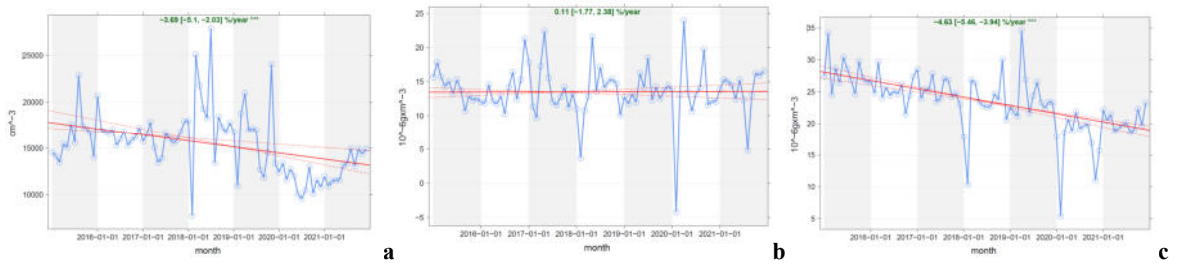

Figure 4a-c. Theil-Sen trend (deseasoned) for monthly means, 2015-2021, from wind from airport: WR 270°-340°, for (a) LAN: TNC, DAR: (b) PM10 and (c) NO2.

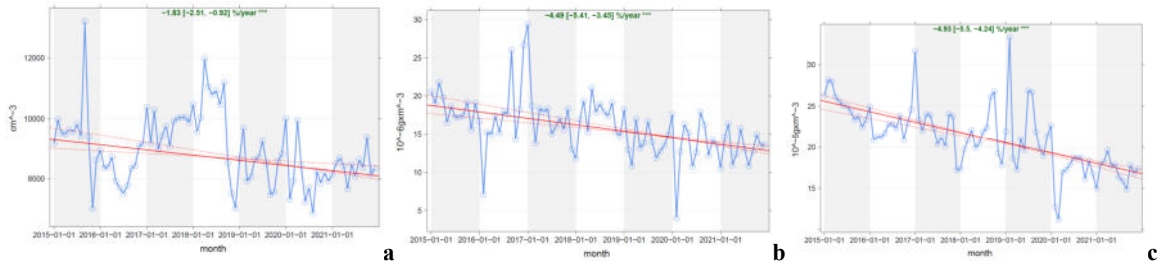

Figure 5a-c. Theil-Sen trend (deseasoned) for monthly means, 2015-2021, from wind not from airport: WR 350°–360° + 0°-260°, for (a) LAN: TNC, DAR: (b) PM10 and (c) NO2.

The airport as an additional source of NUC could be the reason for the lower decline rates compared to the other locations. When only wind from the airport is considered, the trend is higher (-3.7% per year, 2015 to 2021, s. Fig. 4a). Here the pandemic year 2020 shows a dip before increasing again in 2021. This could be due to reduced emissions from the airport. The decrease in wind from the other directions was lower at -1.8% p.a. (Fig. 5a) and showed no visible impact in 2020.

3.3. Influence of sources and meteorological parameters

In this section, we analyse the variations of PNSD and its subfractions as a function of different meteorological variables. For the analysis of the temporal variation of the auxiliary compounds, we focus on the available data from 2019 to 2021.

3.3.1. Influence of wind direction on particle number concentrations

Figure 6 shows the average particle number concentration of all the years included in this analysis for each subfraction of the PNSD as a function of wind direction (aggregated to 10° steps) and wind speed (as distance from the centre). From this figure we can see high concentrations coming from the direction of the airport (NW indicated with a white arrow) with a maximum of 16×10^3 cm^-3 for NUC. However, from this figure alone, it is unclear which factors influence the other size fractions AIT (Fig. 6b) and ACC (Fig. 6c) showing a maximum which could originate from various directions. Therefore, we analyse further by splitting the polar plot into the different years as shown in Fig. 7.

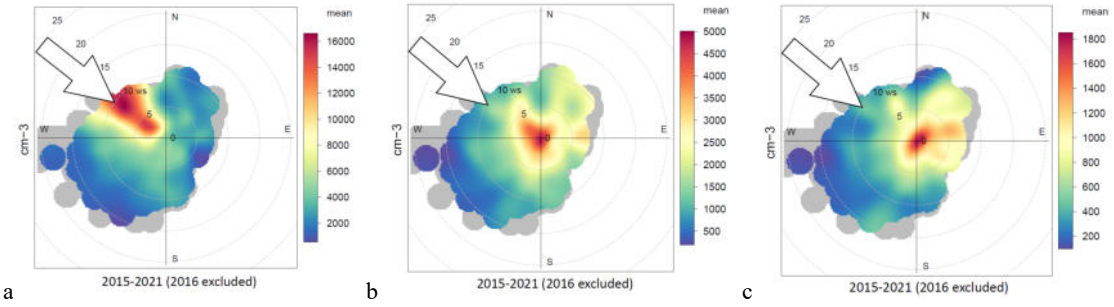

Figure 6. Polarplot for particle number concentration in cm^-3, average of hours of the years 2015-2021 (2016 excluded), in LAN. (a) NUC, (b) AIT and (c) ACC. Grey spots represent cases less than 2 hours. The arrow indicates the wind from the airport.

In 2020 (Fig. 6a), the lowest maximum value of NUC was observed with 7×10^3 cm^-3 from the NW, which was reduced to 50% compared to the average of all previous years. This year also had the lowest air traffic according to the Frankfurt Airport Air Traffic Statistics 2023 (Schultheiß-Münch et al., 2024) (s. 3.2). The maximum increased again in 2021. The highest 10° concentration was measured in 2018 from the NW at 9 m x s^-1 with 20×10^3 cm^-3. In 2021, NW showed lower concentrations of 12×10^3 cm^-3 than in the years before 2020, with 12 – 20×10^3 cm^-3. We conclude that the airport 6 kilometres away has a strong influence on NUC concentrations.

AIT concentrations were highest in three directions: NW, NE, and S, reaching up to 4.5×10^3 cm^-3 at wind speeds of less than 3 m×s^-1. The lowest concentration was observed from the SW with a 10 times lower concentration of 0.5×10^3 cm^-3. Figure 7b depicts the development of the average individual years. The highest concentration was recorded in 2017 from all directions at < 1 mxs^-1, while the lowest concentration was in 2020 with SW winds at 15 m×s^-1.

The highest ACC concentration of 1.6×10^3 cm^-3 was measured from all directions at < 2 m×s^-1. The second-highest concentration was 1.2×10^3 cm^-3 and came from the E at 7 m×s^-1. Figure 7c depicts the development of the average individual years. The maximum was found in 2018 from E at 5 m×s^-1 with 1.8×10^3 cm^-3. The minimum in 2019 and 2020 from SW was < 0.1×10^3 cm^-3.

The 2019–2021 PM concentration polar diagrams in LAN and DAR showed a pattern that was similar to ACC (Fig. S3a, b). The highest concentration was found in the NE quadrant, especially in 2019 and 2021, with wind speeds of 10 m×s^-1 from NNE.

Figure S4 depicts the average NO_2 concentrations in the DAR over different years. Concentrations are highest from the northwest at 10 m×s^-1 and lowest from the southwest at wind speeds ranging from 0.5 to 5 m×s^-1 throughout the years. The NO_2 pattern appears to be partly influenced by the FRA airport, located 18 km away, and local sources. But the highest concentration from NW was not found in 2019 like with NUC, possibly due to the changing ratio between NO_2 and NUC from 2015 to 2019.

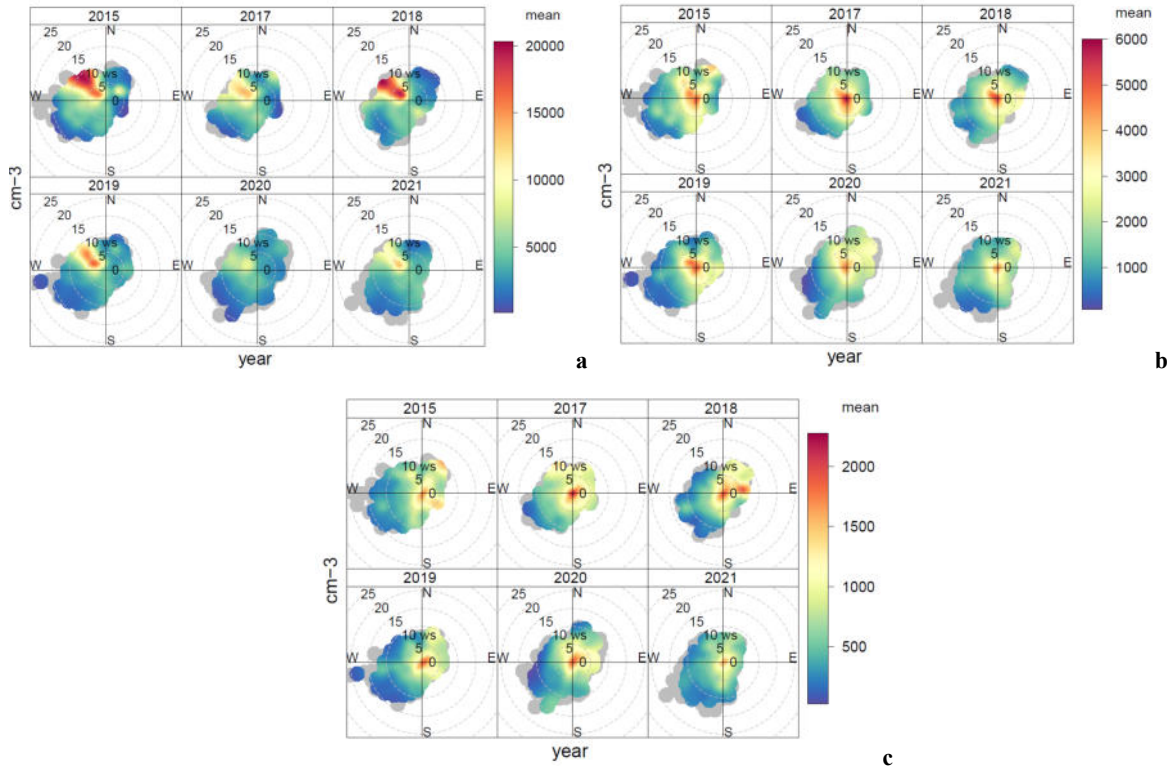

Figure 7: Polarplot for particle number concentration in cm^-3, average of hours separated from 2015 to 2021 (excluding 2016), in LAN. (a) NUC, (b) AIT and (c) ACC. Grey spots represent cases less than 2 hours.

In contrast to NUC, wherein the highest concentration is in the direction of the airport, like in other studies before (Keuken et al., 2015), AIT and ACC showed a different pattern that is not directed towards the airport. These bigger particles could be influenced less by air traffic and more by other sources, such as tailpipe emissions, abrasion and resuspension or long-range transport (Okuljar et al., 2021). We speculate that AIT has sources in

the traffic sector, in line with the arguments of Trechera et al., 2023. We interpret the pattern of ACC to the movement of large-scale meteorological air masses across Central Europe, as described in (Engler et al., 2007). In line with ACC, high PM10 concentrations from NE with higher wind speed point to long-range transport effects (van Pixteren et al., 2019).

3.3.2. Seasonal variability

The annual variation for the entire period of TNC showed a maximum in summer, with the highest concentrations in July and August, and about 20% higher concentrations during May-September compared to the rest of the year. (See Fig. S5, where shaded areas represent 75% and 95% confidence intervals). TNC followed the same pattern as particles < 100 nm, as both NUC and AIT reached their maximums in summer (Jul-Aug). In contrast, ACC did not show pronounced maxima. For a comparison with airport traffic, cf. chapter 3.6.

We found a seasonal variability for PM1, PM2.5 and PM10, with a winter-to-summer ratio of 2-3 for PM2.5 in LAN (Fig. S6). The PM10 concentration in DAR is lower in November and December than in LAN.

The secondary parameter ozone showed its maximum in summer; others such as NO_2, NO and CO showed their maxima in winter (Fig. S7).

For UFP at LAN and gaseous compounds at DAR, we discovered that TNC, NUC, AIT, and ozone have an annual cycle, with the highest concentrations in the summer. In contrast, PM, particularly $PM_{2.5}$, NO_2, NO, and CO, reached their peak in the winter. Possibly due to higher heating emissions and lower MLH in the winter.. Studies have shown that wood combustion is a significant source of particulate matter during winter (Pinxteren, 2016).

3.3.3. Diurnal variation

In this section we analyse diurnal variation of particle number concentrations which are influenced by meteorology (temperature, humidity, wind speed), anthropogenic activities, and biological processes.

In LAN, the overall diurnal variation (Fig. 6a) of TNC showed two intermediate maxima concentrations (08, 21:00). The first occurred between 7 and 9:00 and a very small midday peak at 13:00 (Fig. S5) and the highest peak was seen at 21:00 in the evening. For NUC, a similar shape was observed, but with a more distinct small midday peak at 13:00 and a slightly earlier evening peak at 20:00. Hourly variations of NUC increased with ozone and global radiation (GLO) between 7:00 and 11:00 (see Fig. 8b), particularly in the summer, but less in the spring and autumn. The midday TNC peak was more pronounced in the summer and less so in the spring and autumn, but it was absent in the winter.

Diurnal variations of AIT and ACC showed the highest concentration between 20:00 and 2:00, especially during Friday and Saturday nights (Fig. S5). ACC showed a second maximum between 7:00 and 9:00, during the week, but not on weekends.

In LAN 2019-21, we found diurnal variability for PM1, $PM_{2.5}$, and PM_{10}, with PM_1 having a (Fig. S6) minimum between 15 and 18:00. In contrast, PM10 in DAR showed a profile with a maximum concentration during rush hour at 8:00 and a minimum concentration in the morning hours of 3–4:00. On average, the diurnal variability during 2015–2021 was similar to LAN in 2019–2021.

Ozone showed a midday peak at 15:00 (Fig. S7) and a minimum at 7:00. In contrast, NO, NO_2, and CO showed two peaks at 08–10:00 and 20–22:00 (see Fig. S7 and S8). SO_2 showed the highest concentration between 09:00 and 13:00.

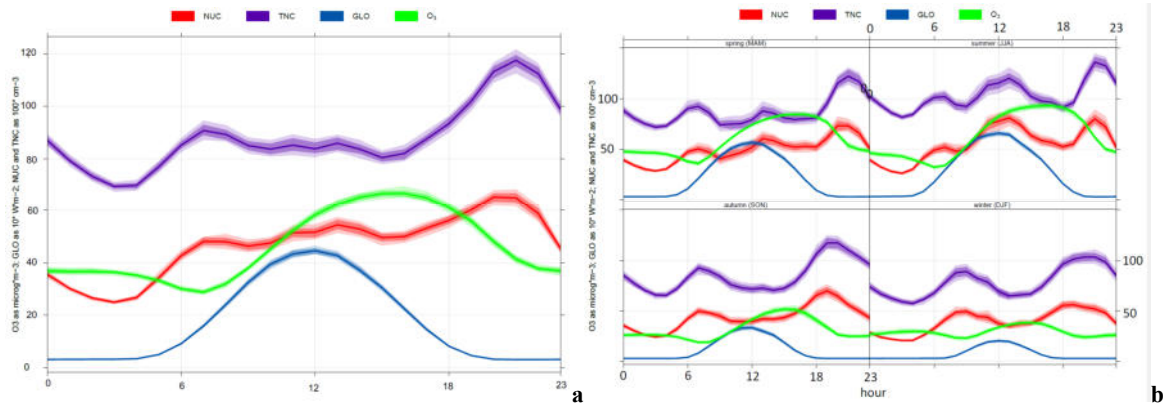

Figure 8. The diurnal variation of hourly means, 2019-2021, NUC, TNC, GLO and O3 in LAN (a); and for the 4 seasons separately (b). Shaded areas represent 75% and 95% confidence intervals.

The TNC concentration showed three peak concentrations. The first is between 7 and 9:00 a.m. during traffic rush hours, which could be due to aircraft activity, as observed in many previous studies (Sun et al., 2019; Trechera et al., 2023). Traffic influence also plays a role,with the highest peak between 6 and 10:00 a.m. (Wehner et al., 2002). In LAN (see Fig. S5), we also observed a small TNC peak during late morning to midday. This midday TNC peak showed lower concentrations than the morning traffic rush hour peak. In contrast, the midday NUC peak exceeded the morning rush hour concentrations. The highest concentrations for both TNC and NUC were found during night hours (21:00-0:00), probably due to nocturnal inversion layers.

The pronounced midday TNC peak is consistent with regional or urban photo-nucleation processes, as well as fumigation from higher atmospheric layers rich in nucleation mode particles and ozone. The MLH grows due to convective dynamics, aviation, and/or power plants. This was observed with a higher midday peak in summer, compared to none in winter (see Fig. 8), which was attributed to photo-nucleation.

ACC showed a peak during morning rush hours on weekdays, indicating that car traffic was the source of this peak. Similarly, NO, NO2 showed higher peaks during rush hours on weekdays than on working weekdays (Fig. S5, S7).

CO showed a pattern for the evening/night peak independently of the weekday day indicating non-traffic sources, but the morning peak was reduced on Saturdays and even vanished on Sundays (Fig. S8).

3.3.4. Weekday variations

On Sundays, NUC (-20%) and TNC (-15%) were reduced compared to working weekdays (Fig. S5). Hourly variations during the week show that the maximum of the afternoon peak varies in relation to the morning peak from weekday to weekend. Diurnal variations of AIT showed the highest concentrations between 20 - 2:00 on Friday and Saturday nights. AIT was highest on Saturdays (Fig. S5). On the weekends, ACC was only slightly higher. We found a day of the week variability for PM10 in LAN and DAR (Fig. S6). Highest concentration on Wednesdays/Thursdays and lowest on Sundays, with a difference of 3 µg×m^-3. PM10 concentrations were similar on Saturdays and Mondays.

NO and NO_2 were highest during the week, with a minimum on Sunday (-25% NO_2). Ozone showed the inverse behaviour, with a maximum on Sunday and lowest during the working days. CO was slightly lower, and SO_2 showed a clearer minimum on Sundays.

We found on Sundays reduced concentrations of NUC, TNC and NO_2 (and less CO). Also, from 2015 to 2021, on average, 54% less traffic was counted at LAN_TC on Sundays than on Tuesdays through Thursdays (BAST,

2023). Therefore, we assume that the number of 10 – 30 nm particles was partly raised by car traffic during working weekdays, besides other causes like NPF. The afternoon NUC peak shifted from weekday to weekend. This might reveal that NUC and TNC were influenced by traffic. It is possible that the NUC-NPF peak in the afternoon is supplemented by the traffic-NUC peak, which decreases after traffic rush hours and is also reduced on Sundays.

Higher concentrations of AIT and, to a lesser extent, ACC, particularly at night before and after Saturday, may indicate the influence of increased barbecue and residential wood heating activity over the weekend in the nearby residential area. This results in higher emissions of these larger particle modes. It is known that the combustion of solid fuels produces distributions with a modal diameter of approximately 100 nm (Hopke et al., 2022), which falls within both AIT and ACC. Wood burning activities are also associated with higher benzene concentrations at 18:00 elsewhere (Hellén et al., 2008).

3.4. Correlation of particle modes with auxiliary pollutants and meteorological parameters 2021

Due to the start of availability for PM in LAN from 2019 on, and because the COVID-19 lockdown caused a reduction in traffic in 2020. Therefore, we focus on the year 2021 to compare different measured parameters with each other. The average concentration of four size modes and PM fractions, meteorological parameters and auxiliary pollutants can be found in Table S3 with a coverage rate between 92 and 100%.

The mean concentrations in DAR in 2021 were PM_{10} 13 µg×m^-3; NO 4 µg×m^-3; NO_2 17 µg×m^-3; CO 0.2 mg×m^-3; SO_2 0.8 µg×m^-3; Ozone 42 µg×m^-3. In LAN: PM_{10} 14 µg×m^-3, $PM_{2.5}$ 10 µg×m^-3 and PM_1 9 µg×m^-3, TNC 8.3×10^3 cm^-3, NUC 4.9×10^3 cm^-3, AIT 2.9×10^3 cm^-3, ACC 1.0×10^3 cm^-3.

The matrix in Fig. S9 shows the correlations between different particle fractions and auxiliary parameters in 2021. The particle number of TNC showed a significantly high to moderate correlation with NUC and AIT (R= 0.90 and R = 0.64) respectively, but a low correlation with ACC (R = 0.26). The LAN PM_{10} correlated highly and significantly with LAN PM_1 and LAN $PM_{2.5}$ (R= 0.73, 0.88) but showed a low negative correlation with NUC (R = -0.08).

NO_2 in DAR correlated moderately with $PM_{2.5}$ but not significantly (R= 0.44) and not with NUC (R=0.09). NO2 correlated highest with CO as another traffic-related pollutant (R= 0.73). SO_2 only correlated very low with NO_2 and PM fractions (R= 0.18 and R= 0.15–0.17). Ozone correlated moderately with temperature and global radiation (R= 0.52, 0.45), but not with any of the particle fractions. Concerning the meteorological parameters, a low positive correlation is obtained for both TNC and NUC (N10-30) with temperature (R= 0.22 to 0.23) and a very low negative correlation with RH (R= -0.06 to -0.09). Negative correlations were also observed for wind speed with all size modes, moderate for AIT and ACC (R = -0.51) and low for NUC (R = -0.11). Using a multiple linear regression approach, temperature and wind speed were two of the six most influential parameters for the spatio-temporal variance of UFP (von Bismarck-Osten et al., 2013).

3.5. Comparison with the WHO classification

According to the WHO definition of UFP, TNC has a lower limit of ≤ 10 nm and no restriction on the upper limit (WHO, 2021). The WHO classifies high concentrations as days > 10,000 cm^-3 or hours > 20,000 cm^-3. We discovered high concentrations in LAN on 23-59% of days and 2-6% of hours per year (see Tab. S 5). The WHO limit for high UFP in 24 hours per year was exceeded on 30% of all days. During the lockdown, there were fewer exceedances (23% per day and 2% of hours) than in previous years (37-59% of days and 5-6%).

Considering the WHO classification for low concentrations per day (< 1,000 cm^-3), no day of the entire measurement campaign was in this category.

These findings are limited to this specific location and time period of campaign. In the future, these results should be compared with data from other stations to further discuss their representativeness for similar station types and other local specific sources.

3.6. Temporal variability of emissions from the airport

To estimate the temporal variability of emissions from air traffic at Frankfurt Airport, we show the variability of flight activity measured in terms of passengers carried (PAX) and aircraft movements such as landings and take-offs (LTO).

Between 2015 and 2019, PAX at FRA averaged 65 million per year and increased by 2% per year (Schultheiß-Münch et al., 2022). PAX fell to 29% in 2020 and 38% in 2021, compared to previous years' averages. The LTO (490,000 on average) declined to 44% / 55% in 2020 / 2021. In 2023, the PAX and LTO were 90% of those in 2015-2019 (Schultheiß-Münch et al., 2024). The 95th percentile of the TNC fell by 25% in spring 2020 compared to the previous year (see Fig. 2) before rising again. In Fig. 3a, the monthly mean values from the airport's wind sector also show a constant average of 17×10^3 cm^-3 in 2015-19. The values fell to 12×10^3 cm^-3 in 2020 and then rose again slightly to 14×10^3 cm^-3. This could also indicate that lower air traffic results in a lower maximum TNC.

The seasonal behaviour in 2023 is expected to be similar to the years preceding 2020. LTO has a seasonal maximum plateau from June to October and a minimum in February, with approximately 70% of the maximum (Schultheiß-Münch et al., 2024). TNC follows a similar pattern to LTO, with a maximum in the summer, highest in July and August, and approximately 20% higher concentrations from May to September compared to the remainder of the year. As a result, this time pattern could also indicate TNC caused by aircraft movements other than the new NPF in the summer (s. 3.3.2).

The LTO's 24-hour fluctuation from 2015 to 2021 is characterised by a ban on night flights between 23 and 5:00 since 2011. Some exceptions exist, such as approximately 3% of the maximum daytime hours in 2019 (Gemeinnützige Umwelthaus GmbH, 2025). In 2019, the LTO is 0% between 0 and 5:00, and 30% from 5:00 to 7:00. Highest between 7 and 22:00 with 80 to 100%: The three maxima are 7-13:00, 16:00, and 20:00, with the lowest at 18-19:00 at 80%. As described in 3.3.3, NUC had a similar shape with three maxima (08, 13, 21:00), but with a clearer small midday peak at 13:00 than TNC did. The TNC midday peak was most noticeable in the summer and completely absent in the winter. Because the LTO diurnal cycle is consistent throughout the year, this midday peak appears to be unaffected by air traffic, or at least less so than the NPF.

Previous short-term studies of UFP near FRA, including spatially resolved measurements (Gregor et al., 2015), demonstrated that FRA is a source of UFP, particularly for small diameters in the NUC range. Atmospheric observations downwind of airports generally show increased UFP, especially in the NUC range (Harrison et al., 2019; Hudda et al., 2014; Keuken et al., 2015). Elsewhere, it is discussed that regional or urban photochemical NPF is not exclusively the cause of the high nucleation mode. An influence of airports is also described (Rivas et al., 2020)

4. Conclusions

- The effect of airport emissions upon the particle number concentration and 3 size classes starting from 10 nm was assessed at a site 6 km downwind from a major European airport (FRA) serving the Metropolitan region Rhine-Main (Frankfurt (Main)).
- Wind-influenced concentration analysis indicates that FRA is a strong potential source for nucleation and partly also for Aitken mode particles in an urban background station downwind from the airport. The average NUC concentrations were 2.5 times higher with wind from the airport than with other wind directions. We therefore draw the conclusion that aircraft emissions from a major airport within a 6-kilometer radius seem to have an impact on NUC.
- We discuss the value of long-term observations in understanding trends and investigating the effects of global events like pandemics on air pollution. In the COVID-19-lockdown-influenced year 2020, with the lowest flight traffic, the maximum TNC from airport direction was reduced to 25% of the previous year's average, the lowest maximum in 6 years.
- The WHO limit for high UFP in 24 hours (> 10,000 cm^-3) per year was exceeded on 30% of all days.

Data availability.

The data that support the findings of this study are available at DOI: 10.5281/zenodo.17083383.

Supplement.

The link to the supplement will be included by Copernicus.

Authorship contribution statement

HG: Conceptualisation, Data Curation, Investigation, Validation, Visualisation, Formal analysis, Methodology, Writing – original draft, Writing – review & editing. WB: Software, Writing – review & editing. KW: Software, Formal analysis, Methodology, Writing – review & editing. HA: Writing – review & editing. AW: Methodology, Writing – review & editing. WT: Supervision, Writing – review & editing.

Competing interests. The contact author has declared that none of the authors have any competing interests.

Acknowledgements

We thank the German Environment Agency (UBA) for providing the measurement infrastructure. Auxiliary data was provided by the German Weather Service (DWD), HLNUG, and BAST. We are grateful for their assistance. Not only that, but we also acknowledge Karin Uhse and Sabrina Unglert for technical support and help with data processing.

References

Anon: Directive - EU - 2024/2881 - EN - EUR-Lex, 2024.

BAST, 2023. BASt - Automatische Straßenverkehrszählung: aktuelle Werte. Fed. Highw. Res. Inst. Personal communication.

Birmili, W., Weinhold, K., Rasch, F., Sonntag, A., Sun, J., Merkel, M., Wiedensohler, A., Bastian, S., Schladitz, A., Löschau, G., Cyrys, J., Pitz, M., Gu, J., Kusch, T., Flentje, H., Quass, U., Kaminski, H., Kuhlbusch, T.A.J., Meinhardt, F., Schwerin, A., Bath, O., Ries, L., Gerwig, H., Wirtz, K., Fiebig, M., 2016. Long-term observations of tropospheric particle number size distributions and equivalent black carbon mass concentrations in the German Ultrafine Aerosol Network (GUAN). Earth Syst. Sci. Data 8, 355–382. https://doi.org/10.5194/essd-8-355-2016

Bousiotis, D., Brean, J., Pope, F.D., Dall'Osto, M., Querol, X., Alastuey, A., Perez, N., Petäjä, T., Massling, A., Nøjgaard, J.K., Nordstrøm, C., Kouvarakis, G., Vratolis, S., Eleftheriadis, K., Niemi, J.V., Portin, H., Wiedensohler, A., Weinhold, K., Merkel, M., Tuch, T., Harrison, R.M., 2021. The effect of meteorological conditions and atmospheric composition in the occurrence and development of new particle formation (NPF) events in Europe. Atmos. Chem. Phys. 21, 3345–3370. https://doi.org/10.5194/acp-21-3345-2021

Brines, M., Dall'Osto, M., Beddows, D.C.S., Harrison, R.M., Gómez-Moreno, F., Núñez, L., Artíñano, B., Costabile, F., Gobbi, G.P., Salimi, F., Morawska, L., Sioutas, C., Querol, X., 2015. Traffic and nucleation events as main sources of ultrafine particles in high-insolation developed world cities. Atmos.Chem. Phys. 15, 5929–5945. https://doi.org/10.5194/acp-15-5929-2015

Brock, C.A., Schröder, F., Kärcher, B., Petzold, A., Busen, R., Fiebig, M., 2000. Ultrafine particle size distributions measured in aircraft exhaust plumes. J. Geophys. Res. Atmospheres 105, 26555–26567. https://doi.org/10.1029/2000JD900360

Carslaw, D.C., Ropkins, K., 2012. openair — An R package for air quality data analysis. Environ. Model. Softw. 27–28, 52–61. https://doi.org/10.1016/j.envsoft.2011.09.008

Cassee, F.R., Morawska, L., Peters, A., 2019. The White Paper on Ambient Ultrafine Particles: evidence for policy makers. 'Thinking outside the box' Team [WWW Document]. URL https://efca.net/files/WHITE%20PAPER-UFP%20evidence%20for%20policy%20makers%20(25%20OCT).pdf (accessed 02.11.26).

CEN, 2023. prEN 16976 - Ambient air - Determination of the particle number concentration of atmospheric aerosol [WWW Document]. ITeh Stand. URL https://standards.iteh.ai/catalog/standards/cen/ab8b1143-a1d3-481b-b268-38a3b1da18b7/pren-16976 (accessed 02.11.26).

CEN, 2020. CEN/TS 17434:2020 - Ambient air - Determination of the particle number size distribution of atmospheric aerosol using a Mobility Particle Size Spectrometer (MPSS) [WWW Document]. ITeh Stand. URL https://standards.iteh.ai/catalog/standards/cen/a841bc08-ed34-4fa8-94ca-8c5e07b99db9/cen-ts-17434-2020 (accessed 02.11.26).

Chen, Y., Masiol, M., Squizzato, S., Chalupa, D.C., Zíková, N., Pokorná, P., Rich, D.Q., Hopke, P.K., 2022. Long-term trends of ultrafine and fine particle number concentrations in New York State: Apportioning between emissions and dispersion. Environ. Pollut. 310, 119797. https://doi.org/10.1016/j.envpol.2022.119797

Cleveland, R.B., Cleveland, W.S., Terpenning, I., 1990. STL: A Seasonal-Trend Decomposition Procedure Based on Loess. J Stat 6, 3–73.

DFS, 2022. Die DFS-Energiezentrale. Transm. Mag. DFS Dtsch. Flugsicherung GmbH.

Emeis, S., Schäfer, K., Münkel, C., 2008. Surface-based remote sensing of the mixing-layer height a review. Meteorol. Z. 621–630. https://doi.org/10.1127/0941-2948/2008/0312

Engler, C., Rose, D., Wehner, B., Wiedensohler, A., Brüggemann, E., Gnauk, T., Spindler, G., Tuch, T., Birmili, W., 2007. Size distributions of non-volatile particle residuals (Dp<800 nm) at a rural site in Germany and relation to air mass origin. Atmos. Chem. Phys. 7, 5785–5802. https://doi.org/10.5194/acp-7-5785-2007

Gani, S., Chambliss, S.E., Messier, K.P., Lunden, M.M., Apte, J.S., 2021. Spatiotemporal profiles of ultrafine particles differ from other traffic-related air pollutants: lessons from long-term measurements at fixed sites and mobile monitoring. Environ. Sci. Atmospheres 1, 558–568. https://doi.org/10.1039/D1EA00058F

Garcia-Marlès, M., Lara, R., Reche, C., Pérez, N., Tobías, A., Savadkoohi, M., Beddows, D., Salma, I., Vörösmarty, M., Weidinger, T., Hueglin, C., Mihalopoulos, N., Grivas, G., Kalkavouras, P., Ondracek, J., Zikova, N., Niemi, J.V., Manninen, H.E., Green, D.C., Tremper, A.H., Norman, M., Vratolis, S., Diapouli, E., Eleftheriadis, K., Gómez-Moreno, F.J., Alonso-Blanco, E., Wiedensohler, A., Weinhold, K., Merkel, M., Bastian, S., Hoffmann, B., Altug, H., Petit, J.-E., Acharja, P., Favez, O., Santos, S.M.D., Putaud, J.-P., Dinoi, A., Contini, D., Casans, A., Casquero-Vera, J.A., Crumeyrolle, S., Bourrianne, E., Poppel, M.V., Dreesen, F.E., Harni, S., Timonen, H., Lampilahti, J., Petäjä, T., Pandolfi, M., Hopke, P.K., Harrison, R.M., Alastuey, A., Querol, X., 2024. Source apportionment of ultrafine particles in urban Europe. Environ. Int. 194, 109149. https://doi.org/10.1016/j.envint.2024.109149

Geiss, A., et al., 2017, 'Mixing layer height as an indicator for urban air quality?', Atmospheric Measurement Techniques 10(8), pp. 2969-2988 (DOI: 10.5194/amt-10-2969-2017).

Gemeinnützige Umwelthaus GmbH, 2025. Flugbewegungen 2024 / Gemeinnützige Umwelthaus GmbH [WWW Document]. Flugbewegungen 2024. URL https://www.umwelthaus.org/fluglaerm/fluglaermmonitoring/monitoring-der-flugbewegungen/flugbewegungen-2024/ (accessed 2.11.26).

Gregor, M., Gerwig, H., Wirtz, K., 2015. High peak concentrations of alveolar lung deposited surface area and particle number during overflights before touchdown [WWW Document]. URL https://geko.promeeting.it/abstract/DEF/Poster/1COA_P017.pdf (accessed 2.11.26).

Harrison, R.M., Beddows, D.C.S., Alam, M.S., Singh, A., Brean, J., Xu, R., Kotthaus, S., Grimmond, S., 2019. Interpretation of particle number size distributions measured across an urban area during the FASTER campaign. Atmos.Chem. Phys. 19, 39–55. https://doi.org/10.5194/acp-19-39-2019

Hellén, H., Hakola, H., Haaparanta, S., Pietarila, H., Kauhaniemi, M., 2008. Influence of residential wood combustion on local air quality. Sci. Total Environ. 393, 283–290. https://doi.org/10.1016/j.scitotenv.2008.01.019

HLNUG, 2023a. Luftmessstelle Darmstadt | Messdatenportal [WWW Document]. Hessian Agency Nat. Conserv. Environ. Geol. URL https://www.hlnug.de/messwerte/datenportal/messstelle/2/1/0104/ (accessed 2.11.26).

HLNUG, 2023b. Emissionskataster [WWW Document]. URL https://www.hlnug.de/themen/luft/emissionen/emissionskataster (accessed 02.11.26).

Hopke, P.K., Feng, Y., Dai, Q., 2022. Source apportionment of particle number concentrations: A global review. Sci. Total Environ. 819, 153104. https://doi.org/10.1016/j.scitotenv.2022.153104

Hudda, N., Gould, T., Hartin, K., Larson, T.V., Fruin, S.A., 2014. Emissions from an International Airport Increase Particle Number Concentrations 4-fold at 10 km Downwind. Environ. Sci. Technol. 48, 6628–6635. https://doi.org/10.1021/es5001566

Hudda, N., Simon, M.C., Zamore, W., Durant, J.L., 2018. Aviation-Related Impacts on Ultrafine Particle Number Concentrations Outside and Inside Residences near an Airport. Environ. Sci. Technol. 52, 1765–1772. https://doi.org/10.1021/acs.est.7b05593

Junkermann, W., Vogel, B., Bangert, M., 2016. Ultrafine particles over Germany – an aerial survey. Tellus B Chem. Phys. Meteorol. 68, 29250. https://doi.org/10.3402/tellusb.v68.29250

Kendall, M.G., 1975. Rank correlation methods, 4th ed., 2d impression. ed. Griffin, London.

Kerminen, V.-M., Chen, X., Vakkari, V., Petäjä, T., Kulmala, M., Bianchi, F., 2018. Atmospheric new particle formation and growth: review of field observations. Environ. Res. Lett. 13, 103003. https://doi.org/10.1088/1748-9326/aadf3c

Keuken, M.P., Moerman, M., Zandveld, P., Henzing, J.S., Hoek, G., 2015. Total and size-resolved particle number an black carbon concentrations in urban areas near Schiphol airport (the Netherlands). Atmos. Environ. 104, 132–142. https://doi.org/10.1016/j.atmosenv.2015.01.015

Languille, B., Gros, V., Petit, J.-E., Honoré, C., Baudic, A., Perrussel, O., Foret, G., Michoud, V., Truong, F., Bonnaire, N., Sarda-Estève, R., Delmotte, M., Feron, A., Maisonneuve, F., Gaimoz, C., Formenti, P., Kotthaus, S., Haeffelin, M., Favez, O., 2020. Wood burning: A major source of Volatile Organic Compounds during wintertime in the Paris region. Sci. Total Environ. 711, 135055. https://doi.org/10.1016/j.scitotenv.2019.135055

Lorentz, H., Janicke, U., Jakobs, H., Schmidt, W., Hellebrandt, P., Ketzel, M., Gerwig, H., 2019. ULTRAFINE PARTICLE DISPERSION MODELLING AT AND AROUND FRANKFURT AIRPORT (FRA), GERMANY [WWW Document]. URL https://www.harmo.org/Conferences/Proceedings/_Bruges/publishedSections/H19-082%20Helmut%20Lorentz.pdf (accessed 02.11.26).

Lupascu, A., Easter, R., Zaveri, R., Shrivastava, M., Pekour, M., Tomlinson, J., Yang, Q., Matsui, H., Hodzic, A., Zhang, Q., and Fast, J. D.: Modeling particle nucleation and growth over northern California during the 2010 CARES campaign, Atmospheric Chemistry and Physics, 15, 12283–12313, https://doi.org/10.5194/acp-15-12283-2015, 2015

Ma, N., et al., 2014, 'Tropospheric aerosol scattering and absorption over central Europe: a closure study for the dry particle state', Atmospheric Chemistry and Physics 14(12), pp. 6241-6259 (DOI: 10.5194/acp-14-6241-2014).

Ma, N., Birmili, W., 2015. Estimating the contribution of photochemical particle formation to ultrafine particle number averages in an urban atmosphere. Sci. Total Environ. 512–513, 154–166. https://doi.org/10.1016/j.scitotenv.2015.01.009

Mann, H.B., 1945. Nonparametric Tests Against Trend. Econometrica 13, 245–259. https://doi.org/10.2307/1907187

Masiol, M., Harrison, R.M., Vu, T.V., Beddows, D.C.S., 2017. Sources of sub-micrometre particles near a major international airport. Atmospheric Chem. Phys. 17, 12379–12403. https://doi.org/10.5194/acp-17-12379-2017

Ohlwein, S., Kappeler, R., Kutlar Joss, M., Künzli, N., Hoffmann, B., 2019. Health effects of ultrafine particles: a systematic literature review update of epidemiological evidence. Int. J. Public Health 64, 547–559. https://doi.org/10.1007/s00038-019-01202-7

Okuljar, M., Kuuluvainen, H., Kontkanen, J., Garmash, O., Olin, M., Niemi, J.V., Timonen, H., Kangasluoma, J., Tham, Y.J., Baalbaki, R., Sipilä, M., Salo, L., Lintusaari, H., Portin, H., Teinilä, K., Aurela, M., Dal Maso, M., Rönkkö, T., Petäjä, T., Paasonen, P., 2021. Measurement report: The influence of traffic and new particle formation on the size distribution of 1–800 nm particles in Helsinki – a street canyon and an urban background station comparison. Atmos. Chem. Phys. 21, 9931–9953. https://doi.org/10.5194/acp-21-9931-2021

Pinxteren, D. van, et al., 2016, 'Regional air quality in Leipzig, Germany: detailed source apportionment of size-resolved aerosol particles and comparison with the year 2000', Faraday Discussions 189(0), pp. 291-315 (DOI: 10.1039/C5FD00228A).

Putaud, J.-P., Pozzoli, L., Pisoni, E., Martins Dos Santos, S., Lagler, F., Lanzani, G., Dal Santo, U., Colette, A., 2021. Impacts of the COVID-19 lockdown on air pollution at regional and urban background sites in northern Italy. Atmos. Chem. Phys. 21, 7597–7609. https://doi.org/10.5194/acp-21-7597-2021

R Core Team, 2019. R: A language and environment for statistical computing. URL. R Foundation for Statistical Computing, Vienna, Austria.

RI-URBANS, 2024. GUIDANCE DOCUMENTS ON MEASUREMENTS & MODELLING OF NOVEL AIR QUALITY POLLUTANTS: ULTRAFINE PARTICLES / SIZE DISTRIBUTIONS [WWW Document]. URL https://riurbans.eu/wp-content/uploads/2024/11/ENV_GUIDANCE-DOCUMENT_ST1_UFP_Definitive.pdf (accessed 2.11.26).

Rivas, I., Beddows, D.C.S., Amato, F., Green, D.C., Järvi, L., Hueglin, C., Reche, C., Timonen, H., Fuller, G.W., Niemi, J.V., Pérez, N., Aurela, M., Hopke, P.K., Alastuey, A., Kulmala, M., Harrison, R.M., Querol, X., Kelly, F.J., 2020. Source apportionment of particle number size distribution in urban background and traffic stations in four European cities. Environ. Int. 135, 105345. https://doi.org/10.1016/j.envint.2019.105345

Schneider, J., et al., 2005, 'Nucleation Particles in Diesel Exhaust: Composition Inferred from In Situ Mass Spectrometric Analysis', Environmental Science & Technology 39(16), pp. 6153-6161 (DOI: 10.1021/es049427m).

Schultheiß-Münch, M., Draxler, H.-A., Jochem, H., 2022. Frankfurt Airport Luftverkehrsstatistik 2021. [WWW Document]. URL https://www.fraport.com/content/dam/fraport-company/documents/investoren/finanz--und-verkehrszahlen/luftverkehrsstatistik/Luftverkehrsstatistik%202021.pdf/_jcr_content/renditions/original./Luftverkehrsstatistik%202021.pdf (accessed 2.11.26).

Schultheiß-Münch, M., et al., 2024, Frankfurt Airport Air Traffic Statistics 2023, Frankfurt a.M. URL https://www.fraport.com/content/dam/fraport-company/documents/investoren/eng/publications/annual-reports/Annual%20Report%202024.pdf/_jcr_content/renditions/original./Annual%20Report%202024.pdf (accessed 2.11.26).

Sen, P.K., 1968. Estimates of the Regression Coefficient Based on Kendall's Tau. J. Am. Stat. Assoc. 63, 1379–1389. https://doi.org/10.2307/2285891

Stacey, B., 2019. Measurement of ultrafine particles at airports: A review. Atmos. Environ. 198, 463–477. https://doi.org/10.1016/j.atmosenv.2018.10.041

Sun, J., Birmili, W., Hermann, M., Tuch, T., Weinhold, K., Merkel, M., Rasch, F., Müller, T., Schladitz, A., Bastian, S., Löschau, G., Cyrys, J., Gu, J., Flentje, H., Briel, B., Asbach, C., Kaminski, H., Ries, L., Sohmer, R., Gerwig, H., Wirtz, K., Meinhardt, F., Schwerin, A., Bath, O., Ma, N., Wiedensohler, A., 2020. Decreasing trends of particle number and black carbon mass concentrations at 16 observational sites in Germany from 2009 to 2018. Atmos. Chem. Phys. 20, 7049–7068. https://doi.org/10.5194/acp-20-7049-2020

Sun, J., Birmili, W., Hermann, M., Tuch, T., Weinhold, K., Spindler, G., Schladitz, A., Bastian, S., Löschau, G., Cyrys, J., Gu, J., Flentje, H., Briel, B., Asbach, C., Kaminski, H., Ries, L., Sohmer, R., Gerwig, H., Wirtz, K., Meinhardt, F., Schwerin, A., Bath, O., Ma, N., Wiedensohler, A., 2019. Variability of black carbon mass concentrations, sub-micrometer particle number concentrations and size distributions: results of the German Ultrafine Aerosol Network ranging from city street to High Alpine locations. Atmos. Environ. 202, 256–268. https://doi.org/10.1016/j.atmosenv.2018.12.029

Theil, H., 1992. A Rank-Invariant Method of Linear and Polynomial Regression Analysis, in: Raj, B., Koerts, J. (Eds.), Henri Theil's Contributions to Economics and Econometrics: Econometric Theory and Methodology, Advanced Studies in Theoretical and Applied Econometrics. Springer Netherlands, Dordrecht, pp. 345–381. https://doi.org/10.1007/978-94-011-2546-8_20

Trechera, P., Garcia-Marlès, M., Liu, X., Reche, C., Pérez, N., Savadkoohi, M., Beddows, D., Salma, I., Vörösmarty, M., Casans, A., Casquero-Vera, J.A., Hueglin, C., Marchand, N., Chazeau, B., Gille, G., Kalkavouras, P., Mihalopoulos, N., Ondracek, J., Zikova, N., Niemi, J.V., Manninen, H.E., Green, D.C., Tremper, A.H., Norman, M., Vratolis, S., Eleftheriadis, K., Gómez-Moreno, F.J., Alonso-Blanco, E., Gerwig, H., Wiedensohler, A., Weinhold, K., Merkel, M., Bastian, S., Petit, J.-E., Favez, O., Crumeyrolle, S., Ferlay, N., Martins Dos Santos, S., Putaud, J.-P., Timonen, H., Lampilahti, J., Asbach, C., Wolf, C., Kaminski, H., Altug, H., Hoffmann, B., Rich, D.Q., Pandolfi, M., Harrison, R.M., Hopke, P.K., Petäjä, T., Alastuey, A., Querol, X., 2023. Phenomenology of ultrafine particle concentrations and size distribution across urban Europe. Environ. Int. 172, 107744. https://doi.org/10.1016/j.envint.2023.107744

Ungeheuer, F., van Pinxteren, D., Vogel, A.L., 2021. Identification and source attribution of organic compounds in ultrafine particles near Frankfurt International Airport. Atmos. Chem. Phys. 21, 3763–3775. https://doi.org/10.5194/acp-21-3763-2021

van Pixteren, D., Mothes, F., Spindler, G., FombA, K.W., Herrmann, H., 2019. Trans-boundary PM10: Quantifying impact and sources during winter 2016/17 in eastern Germany - ScienceDirect. Atmos. Environ. 200, 119–130. https://doi.org/10.1016/j.atmosenv.2018.11.061

von Bismarck-Osten, C., Birmili, W., Ketzel, M., Massling, A., Petäjä, T., Weber, S., 2013. Characterization of parameters influencing the spatio-temporal variability of urban particle number size distributions in four European cities. Atmos. Environ. 77, 415–429. https://doi.org/10.1016/j.atmosenv.2013.05.029

von Schneidemesser, E., Steinmar, K., Weatherhead, E.C., Bonn, B., Gerwig, H., Quedenau, J., 2019. Air pollution at human scales in an urban environment: Impact of local environment and vehicles on particle number concentrations. Sci. Total Environ. 688, 691–700. https://doi.org/10.1016/j.scitotenv.2019.06.309

Vörösmarty, M., Hopke, P.K., Salma, I., 2024. Attribution of aerosol particle number size distributions to main sources using an 11-year urban dataset. Atmospheric Chem. Phys. 24, 5695–5712. https://doi.org/10.5194/acp-24-5695-2024

Wehner, B., Birmili, W., Gnauk, T., Wiedensohler, A., 2002. Particle number size distributions in a street canyon and their transformation into the urban-air background: measurements and a simple model study. Atmos. Environ. 36, 2215–2223. https://doi.org/10.1016/S1352-2310(02)00174-7

Wehner, B., Petäjä, T., Boy, M., Engler, C., Birmili, W., Tuch, T., Wiedensohler, A., and Kulmala, M., 2005: The contribution of sulfuric acid and non-volatile compounds on the growth of freshly formed atmospheric aerosols, Geophysical Research Letters, 32, https://doi.org/10.1029/2005GL023827

WHO, 2021. WHO global air quality guidelines: particulate matter (PM2.5 and PM10), ozone, nitrogen dioxide, sulfur dioxide and carbon monoxide. WHO European Centre for Environment and Health, Bonn, Germany.

Wiedensohler, A., Birmili, W., Nowak, A., Sonntag, A., Weinhold, K., Merkel, M., Wehner, B., Tuch, T., Pfeifer, S., Fiebig, M., Fjäraa, A.M., Asmi, E., Sellegri, K., Depuy, R., Venzac, H., Villani, P., Laj, P., Aalto, P., Ogren, J.A., Swietlicki, E., Williams, P., Roldin, P., Quincey, P., Hüglin, C., Fierz-Schmidhauser, R., Gysel, M., Weingartner, E., Riccobono, F., Santos, S., Grüning, C., Faloon, K., Beddows, D., Harrison, R., Monahan, C., Jennings, S.G., O'Dowd, C.D., Marinoni, A., Horn, H.-G., Keck, L., Jiang, J., Scheckman, J., McMurry, P.H., Deng, Z., Zhao, C.S., Moerman, M., Henzing, B., de Leeuw, G., Löschau, G., Bastian, S., 2012. Mobility particle size spectrometers: harmonization of technical standards and data structure to facilitate high quality long-term observations of atmospheric particle number size distributions. Atmos. Meas. Tech. 5, 657–685. https://doi.org/10.5194/amt-5-657-2012

Wiedensohler, A., Wiesner, A., Weinhold, K., Birmili, W., Hermann, M., Merkel, M., Müller, T., Pfeifer, S., Schmidt, A., Tuch, T., Velarde, F., Quincey, P., Seeger, S., Nowak, A., 2018. Mobility particle size spectrometers: Calibration procedures and measurement uncertainties. Aerosol Sci. Technol. 52, 146–164. https://doi.org/10.1080/02786826.2017.1387229

Yao, L., Garmash, O., Bianchi, F., Zheng, J., Yan, C., Kontkanen, J., Junninen, H., Mazon, S.B., Ehn, M., Paasonen, P., Sipilä, M., Wang, M., Wang, X., Xiao, S., Chen, H., Lu, Y., Zhang, B., Wang, D., Fu, Q., Geng, F., Li, L., Wang, H., Qiao, L., Yang, X., Chen, J., Kerminen, V.-M., Petäjä, T., Worsnop, D.R., Kulmala, M., Wang, L., 2018. Atmospheric new particle formation from sulfuric acid and amines in a Chinese megacity. Science 361, 278–281. https://doi.org/10.1126/science.aao4839

Yu, F., et al., 1999, 'The possible role of organics in the formation and evolution of ultrafine aircraft particles', Journal of Geophysical Research: Atmospheres 104(D4), pp. 4079-4087 (DOI: 10.1029/1998JD200062).

Zhang, X., Karl, M., Zhang, L., Wang, J., 2020. Influence of Aviation Emission on the Particle Number Concentration near Zurich Airport. Environ. Sci. Technol. 54, 14161–14171. https://doi.org/10.1021/acs.est.0c02249